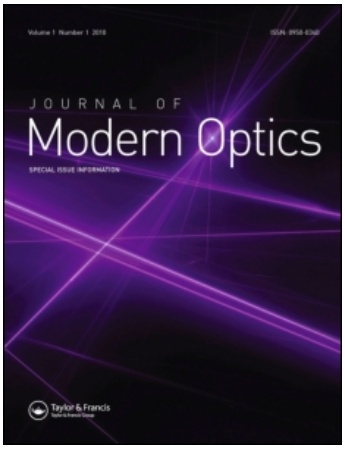

Journal of Modern Optics
Publication details, including instructions for authors and subscription information:
http://www.informaworld.com/smpp/title~content=t713191304

Resolution in Diffraction-limited Imaging, a Singular Value Analysis

M. Bertero[a]; P. Boccacci[b]; E. R. Pike[c]
[a] Istituto Matematico dell'Università and Istituto Nazionale di Fisica Nucleare, Genova, Italy. [b] Istituto di Mineralogia dell'Università, Genova, Italy. [c] Royal Signals and Radar Establishment, Malvern, England.

To cite this Article Bertero, M. , Boccacci, P. and Pike, E. R.(1982) 'Resolution in Diffraction-limited Imaging, a Singular Value Analysis', Journal of Modern Optics, 29: 12, 1599 — 1611
To link to this Article: DOI: 10.1080/713820807
URL: http://dx.doi.org/10.1080/713820807

OPTICA ACTA, 1982, VOL. 29, NO. 12, 1599–1611

Resolution in diffraction-limited imaging, a singular value analysis

II. The case of incoherent illumination

M. BERTERO
Istituto Matematico dell'Università and
Istituto Nazionale di Fisica Nucleare, Genova, Italy

P. BOCCACCI
Istituto di Mineralogia dell'Università, Genova, Italy

and E. R. PIKE
Royal Signals and Radar Establishment, Malvern, England

(*Received 20 April 1982; revision received 2 June 1982*)

Abstract. In a previous paper, methods of singular function expansions have been applied to the analysis of coherent imaging when the object and image domains are allowed to differ. In this paper the method is extended to incoherent illumination, restricting the analysis to the aberration-free case.

While singular functions and singular values for coherent imaging are related in a simple way to the prolate spheroidal functions and their eigenvalues, such relations do not exist for the incoherent imaging case. In spite of this difficulty many properties of singular functions and singular values are derived in this paper and asymptotic estimates are obtained in the limit of large space-bandwidth product. For small values of the space-bandwidth product, the singular values are computed numerically and by means of these results it is shown that super-resolution, in the sense of improving on previous criteria in the presence of noise, can be achieved.

1. Introduction

In a previous paper [1], the theory of coherent imaging has been formulated in terms of singular function expansions in order to allow object and image domains to differ. In such a way it is proved that super-resolution, in the sense of resolution beyond the Rayleigh limit, is possible at low Shannon numbers. In this paper the analysis is extended to the incoherent case. However, whereas for coherent illumination the singular functions can be expressed in terms of the familiar prolate spheroidal functions (even in the presence of phase aberrations) and the singular values are given by the square roots of their eigenvalues, in the incoherent case the situation is more involved. In particular, singular values and singular functions depend on phase aberrations, and for this reason we consider mainly the aberration-free case.

As in [1], for the purposes of clarity, we treat especially the one-dimensional case. We outline the extension to arbitrary pupils in two dimensions but we give numerical results only for the square pupil. Indeed, the determination of singular values requires non-trivial and time-consuming numerical computations.

In the one-dimensional case and in the absence of aberrations and noise, assuming the magnification to be equal to unity without loss of generality, the problem of object restoration is equivalent to the inversion of the integral operator A given by

$$(Af)(x)=\int_{-X/2}^{X/2}\frac{\sin^2[\Omega(x-y)]}{\pi\Omega(x-y)^2}f(y)\,dy,\quad |x|\leqslant X/2. \tag{1.1}$$

Indeed, if $\bar{f}$ is the spatial radiance distribution in the object plane, then $\bar{g}=A\bar{f}$ is the noise-free image in the geometrical region. The function

$$\hat{S}(\omega)=\int_{-\infty}^{+\infty}\frac{\sin^2(\Omega x)}{\pi\Omega x^2}\exp(-i\omega x)\,dx=\left(1-\frac{|\omega|}{2\Omega}\right)\mathrm{rect}\left(\frac{\omega}{2\Omega}\right) \tag{1.2}$$

is the normalized optical transfer function of the system [2]. Here, by rect(t) we denote the function which is 1 when $|t|\leqslant 1$ and 0 when $|t|>1$. Equation (1.2) implies that, if the noise-free image $\bar{g}$ is continued over the whole image space, then its Fourier transform is zero outside $[-2\Omega, 2\Omega]$. This corresponds to the well-known fact that the bandwidth for incoherent imaging is twice the bandwidth for coherent imaging. As a consequence, the Nyquist distance for the analytically continued image g is one-half the Rayleigh resolution distance $R=\pi/\Omega$.

It is convenient to introduce the variables $t=2x/X$ and $c=X\Omega/2$, under which transformation equation (1.1) becomes

$$(Af)(t)=\int_{-1}^{1}\frac{\sin^2[c(t-s)]}{\pi c(t-s)^2}f(s)\,ds,\quad |t|\leqslant 1. \tag{1.3}$$

The operator A is self-adjoint, non-negative, injective and compact in $L^2(-1,1)$; its trace is the Shannon number

$$S=\frac{2c}{\pi}=\frac{X\Omega}{\pi}=\frac{X}{R}. \tag{1·4}$$

Let us denote by λ_k the eigenvalues of A, and by ϕ_k the corresponding normalized eigenfunctions:

$$A\phi_k=\lambda_k\phi_k,\quad \int_{-1}^{1}|\phi_k(t)|^2\,dt=1. \tag{1.5}$$

Then, from the previously stated properties of A it follows that all the eigenvalues of A are strictly positive and that the set of corresponding eigenfunctions form a basis in $L^2(-1,1)$. More precise properties have been derived and numerical computations of the λ_k, ϕ_k have been made [3–5]. The main results are the following: all the eigenvalues of the operator A are non-degenerate and, if they are ordered in a decreasing sequence, then they tend to decrease almost linearly with respect to the order index when $k<4c/\pi$, while for $k>4c/\pi$ they go to zero exponentially fast. When c is sufficiently large (c is proportional to the space-bandwidth product) an approximate formula for the eigenvalues in the case $k<4c/\pi$ is

$$\lambda_k\sim 1-\frac{\pi k}{4c}. \tag{1.6}$$

This approximation is in agreement with a general result obtained by Szegö [6, 7] on Toeplitz operators (see the Appendix).

Now, the solution of the integral equation $A\bar{f}=\bar{g}$, where $\bar{g}$ denotes the noise-free image in the geometrical region $|t|\leqslant 1$, is given by

$$\bar{f}(t)=\sum_{k=0}^{+\infty}\frac{\bar{g}_k'}{\lambda_k}\phi_k(t), \tag{1.7}$$

where

$$\bar{g}_k'=\int_{-1}^{1}\bar{g}(t)\phi_k(t)\,dt. \tag{1.8}$$

As the object size reduces, this approach is not the most convenient since, as noted in [1], in the presence of out-of-band noise the information content of the entire diffracted image is not equivalent to the information content of the geometrical region.

2. Singular values and singular functions for incoherent imagery

Let us suppose now that the noise-free image $\bar{g}$ is known on a region much greater than the geometrical one, so that we can assume without a significant error that it is known from $-\infty$ to $+\infty$. Then let us denote by K the integral operator which continues A, equation (1.3), over the whole image space

$$(Kf)(t)=\int_{-1}^{1}\frac{\sin^2[c(t-s)]}{\pi c(t-s)^2}f(s)\,ds, \quad -\infty<t<+\infty. \tag{2.1}$$

It is convenient to consider K as an operator from $L^2(-1,1)$ into $L^2(-\infty,+\infty)$; it is injective and its range is dense in $\mathscr{B}$, the space of band-limited functions whose Fourier transform is supported in $[-2c, 2c]$.

The adjoint operator K^* is given by

$$(K^*g)(t)=\int_{-\infty}^{+\infty}\frac{\sin^2[c(t-s)]}{\pi c(t-s)^2}g(s)\,ds, \quad |t|\leqslant 1. \tag{2.2}$$

K^* is continuous but not injective; its null space is the orthogonal complement of $\mathscr{B}$, i.e. the subspace of the L^2 functions whose Fourier transform is zero on $[-2c, 2c]$.

By elementary computations we obtain

$$(K^*Kf)(t)=\int_{-1}^{1}H(t-s)f(s)\,ds, \quad |t|\leqslant 1, \tag{2.3}$$

where

$$\begin{aligned}H(t)&=\int_{-\infty}^{+\infty}\frac{\sin^2[c(t-s)]}{\pi c(t-s)^2}\,\frac{\sin^2(cs)}{\pi cs^2}\,ds\\&=\frac{1}{2\pi}\int_{-2c}^{2c}\left(1-\frac{|\omega|}{2c}\right)^2\exp(it\omega)\,d\omega\\&=\frac{c}{2\pi}\,\frac{2ct-\sin(2ct)}{(ct)^3}.\end{aligned} \tag{2.4}$$

Here the convolution theorem for the Fourier transform and equation (1.2) have been used.

The operator (2.3), (2.4) is self-adjoint, non-negative, injective and compact in $L^2(-1,1)$. From these properties it follows that all the eigenvalues of K^*K (let us

denote these eigenvalues by α_k^2) are positive and that the set of the associated eigenfunctions u_k

$$K^*Ku_k = \alpha_k^2 u_k, \quad k = 0, 1, 2, \ldots \tag{2.5}$$

is a basis in $L^2(-1, 1)$. Then one can introduce the singular system [8] $\{\alpha_k; u_k, v_k\}_{k=0}^{+\infty}$ of the operator K, which consists of the solutions of the coupled equations

$$Ku_k = \alpha_k v_k, \quad K^*v_k = \alpha_k u_k. \tag{2.6}$$

The set $\{v_k\}_{k=0}^{+\infty}$ is a basis in $\mathscr{B}$, i.e. in the closure of the range of K. The previous results imply that any object $\bar{f}$ can be expanded as a series of the u_k, while any noise-free image $\bar{g}$ can be expanded as a series of the v_k.

More precise properties of the singular values α_k can be derived by remarking that the operator (2.3), (2.4) is a Toeplitz operator. Indeed, by means of the change of variable $x = ct$, we see that the operator (2.3), (2.4) is of the type (A 1) with

$$\hat{T}(\omega) = \left(1 - \frac{1}{2}|\omega|\right)^2 \operatorname{rect}\left(\frac{\omega}{2}\right). \tag{2.7}$$

A first result on Toeplitz operators is the following [5]: if the function $\hat{L}(\omega) = \omega\hat{T}'(\omega)$ is non-negative (or non-positive) for any value of ω, then all the eigenvalues of the corresponding operator T_c in equation (A 1) are non degenerate. From equation (2.7) it follows that $\omega\hat{T}'(\omega) \leqslant 0$, and therefore *all the eigenvalues α_k^2 of K^*K are non-degenerate.*

As usual, we can assume that the eigenvalues α_k^2 are ordered in a decreasing sequence: $\alpha_0^2 > \alpha_1^2 > \alpha_2^2 > \ldots$. Since K^*K is compact, α_k^2 tends to zero when k tends to infinity. A more precise behaviour for large values of k is given by results of Hille and Tamarkin [9]: since the kernel $T(x)$ is analytic, then the eigenvalues α_k^2 tend to zero exponentially fast.

Now, from the general results on Toeplitz operators quoted in the Appendix, and from equation (2.7), it follows that, for large values of c and for $k < 4c/\pi$, the following approximate expression of the singular values α_k holds:

$$\alpha_k \sim 1 - \frac{\pi k}{4c}. \tag{2.8}$$

By comparing with equation (1.6) we see that, for large values of c, $\alpha_k \sim \lambda_k$; as a consequence it is expected that in such a case no significant improvement in resolution is obtained by using the full image instead of its restriction to the geometrical region. It must be remarked that the approximate equality $\alpha_k \sim \lambda_k$ is already rather well satisfied for moderate values of c, as is shown in figure 1 for $c = 10$, even if the approximate expressions (1.6) and (2.8) (the full line in figure 1) are not yet very accurate. Besides, figure 1 clearly shows that for $c = 10$ only a small amount of out-of-band extrapolation is possible, so that no significant improvement in resolution is expected.

The situation is more favourable when $c < 10$. In table 1 we give for comparison the eigenvalues λ_k and the singular values α_k for $c = 1, 2, 3$. These values have been computed by approximating the kernels of the operators A and K^*K by tensor products of splines [10]. As is evident from table 1, the singular values α_k are considerably greater than the eigenvalues λ_k. Thus, as can be seen in figure 2, where eigenvalues, singular values and asymptotic estimates (1.6), (2.8) are graphically

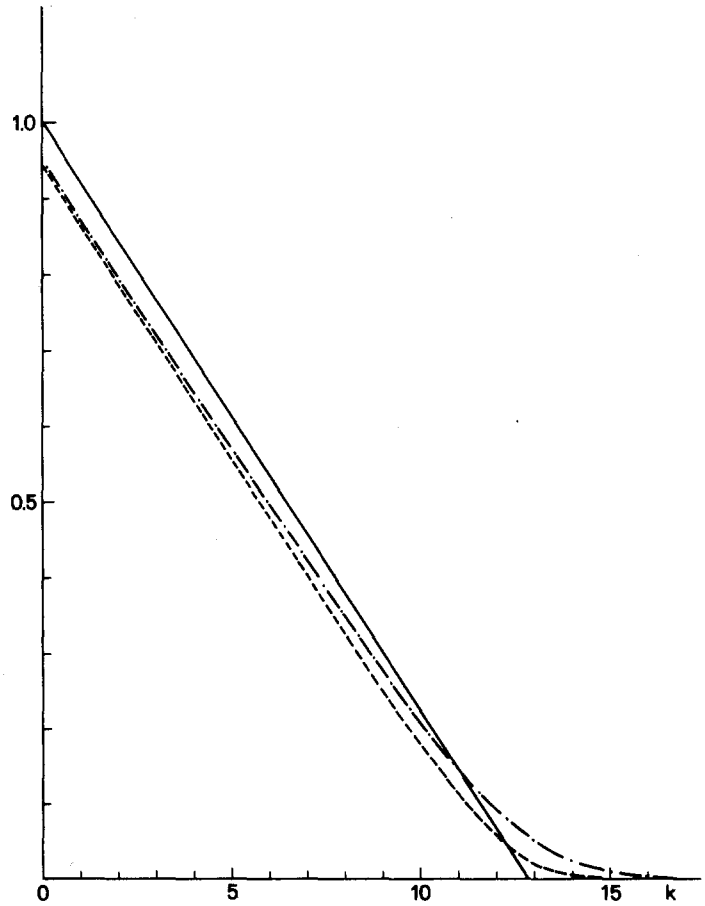

Figure 1. Eigenvalues λ_k (dashed line) and singular values α_k (dash-dotted line) compared with the approximate expression $\mu_k = 1 - \pi k/4c$ (full line) in the case $c = 10$.

Table 1. Eigenvalues λ_k (geometrical image) and singular values α_k (complete image) for incoherent imaging.

	$c=1$		$c=2$		$c=3$	
k	λ_k	α_k	λ_k	α_k	λ_k	α_k
0	$5{\cdot}25\times10^{-1}$	$6{\cdot}14\times10^{-1}$	$7{\cdot}35\times10^{-1}$	$7{\cdot}67\times10^{-1}$	$8{\cdot}18\times10^{-1}$	$8{\cdot}34\times10^{-1}$
1	$1{\cdot}04\times10^{-1}$	$2{\cdot}13\times10^{-1}$	$3{\cdot}89\times10^{-1}$	$4{\cdot}57\times10^{-1}$	$5{\cdot}71\times10^{-1}$	$6{\cdot}06\times10^{-1}$
2	$7{\cdot}48\times10^{-3}$	$4{\cdot}90\times10^{-2}$	$1{\cdot}27\times10^{-1}$	$2{\cdot}15\times10^{-1}$	$3{\cdot}41\times10^{-1}$	$3{\cdot}95\times10^{-1}$
3	$2{\cdot}16\times10^{-4}$	$7{\cdot}66\times10^{-3}$	$1{\cdot}94\times10^{-2}$	$7{\cdot}31\times10^{-2}$	$1{\cdot}42\times10^{-1}$	$2{\cdot}13\times10^{-1}$
4	$3{\cdot}46\times10^{-6}$	$9{\cdot}26\times10^{-4}$	$1{\cdot}45\times10^{-3}$	$1{\cdot}87\times10^{-2}$	$3{\cdot}28\times10^{-2}$	$8{\cdot}99\times10^{-2}$
5	$3{\cdot}45\times10^{-8}$	$8{\cdot}94\times10^{-5}$	$6{\cdot}24\times10^{-5}$	$3{\cdot}73\times10^{-3}$	$3{\cdot}96\times10^{-3}$	$2{\cdot}92\times10^{-2}$
6	—	$7{\cdot}30\times10^{-6}$	$1{\cdot}81\times10^{-6}$	$6{\cdot}22\times10^{-4}$	$2{\cdot}89\times10^{-4}$	$7{\cdot}67\times10^{-3}$
7	—	$5{\cdot}03\times10^{-7}$	$3{\cdot}75\times10^{-8}$	$8{\cdot}81\times10^{-5}$	$1{\cdot}43\times10^{-5}$	$1{\cdot}68\times10^{-3}$
8	—	—	—	$1{\cdot}09\times10^{-5}$	$5{\cdot}30\times10^{-7}$	$3{\cdot}20\times10^{-4}$
9	—	—	—	$1{\cdot}21\times10^{-6}$	$1{\cdot}52\times10^{-8}$	$5{\cdot}37\times10^{-4}$
10	—	—	—	$1{\cdot}25\times10^{-7}$	—	$8{\cdot}10\times10^{-6}$
11	—	—	—	—	—	$1{\cdot}10\times10^{-6}$
12	—	—	—	—	—	$1{\cdot}39\times10^{-7}$

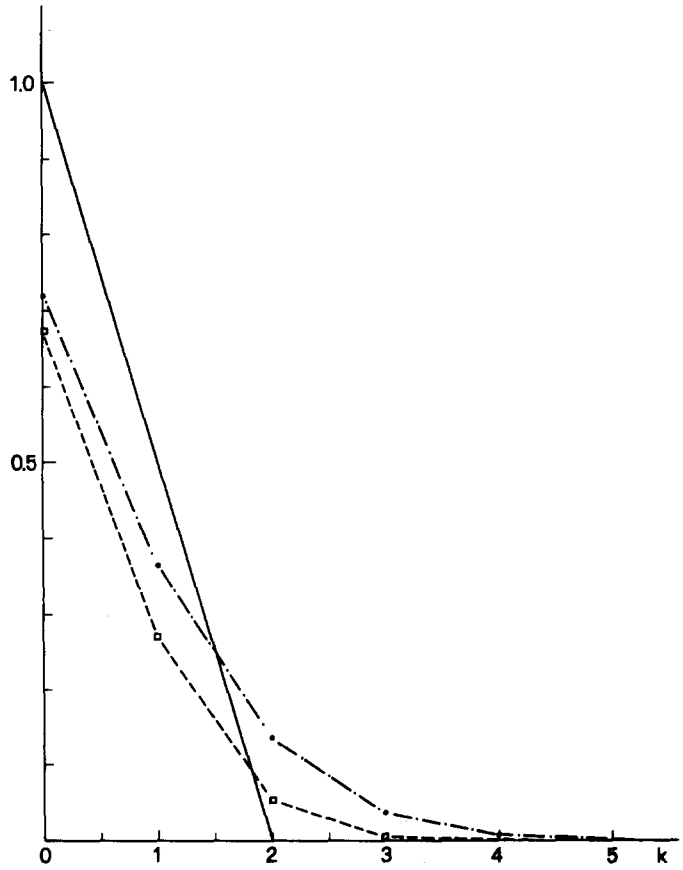

Figure 2. Eigenvalues λ_k (dashed line) and singular values α_k (dash-dotted line) compared with the approximate expression $\mu_k = 1 - \pi k/4c$ (full line) in the case $c = \pi/2$.

represented for $c = \pi/2$, a considerable amount of out-of-band extrapolation is possible, especially using the singular value method.

3. Resolution limits

In terms of the singular system $\{\alpha_k; u_k, v_k\}_{k=0}^{+\infty}$ discussed in § 2, the solution of the integral equation $K\bar{f} = \bar{g}$, where $\bar{g}$ is the full noise-free image, is

$$\bar{f}(t) = \sum_{k=0}^{+\infty} \frac{\bar{g}_k}{\alpha_k} u_k(t), \tag{3.1}$$

where

$$\bar{g}_k = \int_{-\infty}^{+\infty} \bar{g}(t) v_k(t)\, dt. \tag{3.2}$$

Equations (1.7) and (3.2) of this paper correspond respectively to equations (3.17) and (3.14) of [1]. Now, in the coherent case there exists a simple relation between the components $\bar{g}_k$ of the noise-free full image and the components $\bar{g}'_k$ of the same image restricted to the geometrical region (see equation (3.18) of [1]). As a consequence, in

the absence of noise the singular function method and the eigenfunction method are equivalent. No simple relation between $\bar{g}_k$ and $\bar{g}'_k$ can be found in the incoherent case but, in spite of this fact, it is still possible to prove that the solutions (1.7) and (3.1) coincide. This result is a simple consequence of the uniqueness of analytic continuation. Indeed, in the absence of noise the image $\bar{g}$ is band-limited and therefore analytic. It follows that knowledge of $\bar{g}$ in the geometrical region implies the knowledge of $\bar{g}$ everywhere, so that the coefficients $\bar{g}_k$ are uniquely determined by the coefficients $\bar{g}'_k$, and vice versa. This argument also suggests that, as in the coherent case, knowledge of the image out of the geometrical region can become important only in the presence of out-of-band noise.

The analysis of the effect of noise on inversion, as performed in [1], can be immediately extended to the present case. Therefore we give only a very short sketch of this analysis here.

Let us assume that the noise-free image $\bar{g}$ is corrupted by additive noise.

$$g(t)=\bar{g}(t)+n(t), \tag{3.3}$$

where $n(t)$ is a white noise process with power spectrum ε^2; besides, let us assume also that the object $\bar{f}$ is a white noise process with power spectrum E^2. Then, in the eigenfunction method, we can determine only the components of the object corresponding to eigenvalues satisfying the condition

$$\lambda_k \geqslant \varepsilon/E \tag{3.4}$$

while, in the singular function method, we can determine only the components of the object corresponding to singular values satisfying the condition

$$\alpha_k \geqslant \varepsilon/E. \tag{3.5}$$

Now, remarking that both the λ_k and the α_k are ordered in a decreasing sequence, let k_E and k_S be the largest of the values of the index k satisfying condition (3.4) and condition (3.5) respectively. Then $M_E=k_E+1$ is the number of components determined by means of the eigenfunction method, while $M_S=k_S+1$ is the number of components determined by means of the singular function method. From the numerical results reported in § 2, it follows that $M_E<M_S$, although the ratio $(M_S-M_E)/M_S$ decreases as the parameter c increases; in other words, for large values of c the conditions (3.4) and (3.5) become approximately equivalent.

Now, it can be shown by numerical computations that both the eigenfunction ϕ_k and the singular function u_k have exactly k zeros in $[-1, 1]$. As a consequence, one can extend to the present case the arguments developed in [1] and take as a reasonable measure of the resolution achieved by means of the singular function method the quantity $D_S=2/M_S$; then the number of resolution elements contained in the Rayleigh resolution distance R is

$$\frac{R}{D_S}=\left(\frac{\pi}{2c}\right)M_S. \tag{3.6}$$

The number of components M_S and the corresponding number of resolution elements R/D_S can be easily obtained from the singular values of the operator K. The latter have been determined by computing numerically the eigenvalues of the operator K^*K, as we have indicated in § 2. We have used a linear interpolation between adjacent singular values in order to obtain a smooth behaviour of the

parameters M_S and R/D_S as functions of the signal-to-noise ratio E/ε and of the space-bandwidth product c. Some results are given in table 2, and a graphical representation is shown in figure 3.

Table 2. Number of components, M_S, and corresponding number of resolution elements within the Rayleigh distance, R/D_S, restored by the singular value method, as a function of 'signal-to-noise ratio', E/ε; linear case.

$\frac{E}{\varepsilon}$	$c=1$		$c=2$		$c=3$		$c=4$		$c=5$	
	M_S	R/D_S	M_S	R/D_S	M_S	R/D_S	M_S	R/D_S	M_S	R/D_S
10^2	3·94	6·19	5·58	4·38	6·89	3·61	8·26	3·24	9·62	3·02
10^4	5·99	9·40	7·98	6·27	9·83	5·15	11·43	4·49	12·89	4·05
10^6	7·93	12·46	10·19	8·01	12·11	6·34	13·94	5·47	15·73	4·94

$\frac{E}{\varepsilon}$	$c=6$		$c=7$		$c=8$		$c=9$		$c=10$	
	M_S	R/D_S	M_S	R/D_S	M_S	R/D_S	M_S	R/D_S	M_S	R/D_S
10^2	10·87	2·85	12·14	2·72	13·49	2·65	14·75	2·57	15·95	2·51
10^4	14·43	3·78	15·84	3·55	17·23	3·38	18·69	3·26	19·96	3·14
10^6	17·29	4·53	18·87	4·23	20·48	4·02	21·92	3·83	23·50	3·69

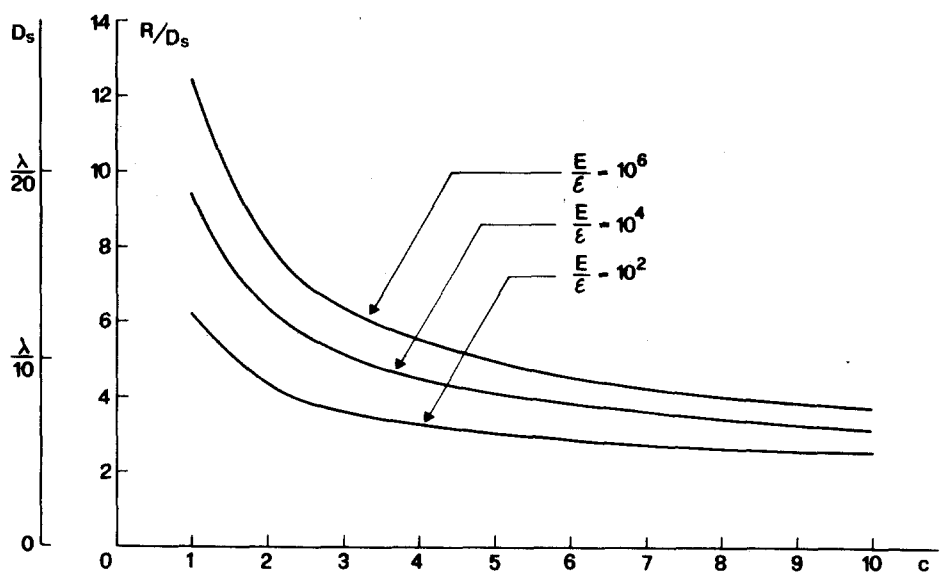

Figure 3. Super-resolution gain using singular value method on complete image for various values of signal-to-noise ratio E/ε; linear case. The scale on the extreme left shows the linear resolution possible with $R=\lambda/2$.

4. The two-dimensional case

We sketch here the extension of the singular function method to the two-dimensional case; we consider only the aberration-free case.

First, a few words about notation. We denote by $\mathbf{x}=\{x_1, x_2\}$ a point in the object or image plane, and by $\omega=\{\omega_1, \omega_2\}$ a point in Fourier space. Then, let $\mathscr{D}$ be the bounded domain containing the support of the object f, and let $\mathscr{A}$ be the bounded domain in Fourier space corresponding to the frequencies which are transmitted by the instrument in the case of coherent illumination. Finally we denote by $E_{\mathscr{A}}$ the characteristic function of $\mathscr{A}$, i.e. the function which is 1 when $\omega\in\mathscr{A}$ and 0 when $\omega\notin\mathscr{A}$, and by $\alpha_{\mathscr{A}}$ the normalized autocorrelation function of $E_{\mathscr{A}}$

$$\alpha_{\mathscr{A}}(\omega)=\frac{1}{m(\mathscr{A})}\int\int_{-\infty}^{+\infty} E_{\mathscr{A}}(\omega+\mu)E_{\mathscr{A}}(\mu)\,d\mu, \tag{4.1}$$

where $m(\mathscr{A})$ is the measure of $\mathscr{A}$. For instance, in the case of a square pupil $\mathscr{A}=[-\Omega,\Omega]\times[-\Omega,\Omega]$, one has

$$\alpha_{\mathscr{A}}(\omega)=\left(1-\frac{|\omega_1|}{2\Omega}\right)\left(1-\frac{|\omega_2|}{2\Omega}\right)\mathrm{rect}\left(\frac{\omega_1}{2\Omega}\right)\mathrm{rect}\left(\frac{\omega_2}{2\Omega}\right), \tag{4.2}$$

while for a circular pupil, $\mathscr{A}$ being the circle of radius Ω, one has

$$\alpha_{\mathscr{A}}(\omega)=\frac{2}{\pi}\left\{\cos^{-1}\left(\frac{|\omega|}{2\Omega}\right)-\left(\frac{|\omega|}{2\Omega}\right)\sqrt{\left[1-\left(\frac{|\omega|}{2\Omega}\right)^2\right]}\right\}E_{\mathscr{A}}\left(\frac{\omega}{2}\right). \tag{4.3}$$

Now, in the case of incoherent illumination, the normalized optical transfer function of the system coincides with the normalized autocorrelation function of $E_{\mathscr{A}}$ and therefore the point-spread function is given by

$$S(\mathbf{x})=\frac{1}{(2\pi)^2}\int\int_{-\infty}^{+\infty}\alpha_{\mathscr{A}}(\omega)\exp\left[i(\mathbf{x},\omega)\right]d\omega. \tag{4.4}$$

When the support of f is contained in $\mathscr{D}$ and the full diffracted image is supposed to be known, the problem of object restoration takes the mathematical expression of the inversion of the integral operator:

$$(Kf)(\mathbf{x})=\int\int_{\mathscr{D}} S(\mathbf{x}-\mathbf{y})f(\mathbf{y})\,d\mathbf{y},\quad \mathbf{x}\in\mathbb{R}^2. \tag{4.5}$$

K is a compact and injective operator from $L^2(\mathscr{D})$ into $L^2(\mathbb{R}^2)$; its range is dense in the subspace $\mathscr{B}_{\mathscr{A}}$ of the band-limited functions whose Fourier transform has a support contained in the support of the normalized autocorrelation function $\alpha_{\mathscr{A}}$. The adjoint operator K^* is given by

$$(K^*g)(\mathbf{x})=\int\int_{-\infty}^{+\infty} S(\mathbf{x}-\mathbf{y})g(\mathbf{y})\,d\mathbf{y},\quad \mathbf{x}\in\mathscr{D}, \tag{4.6}$$

and its null space coincides with the orthogonal complement of $\mathscr{B}_{\mathscr{A}}$; finally K^*K takes the form

$$(K^*Kf)(\mathbf{x})=\int\int_{\mathscr{D}} H(\mathbf{x}-\mathbf{y})f(\mathbf{y})\,d\mathbf{y},\quad \mathbf{x}\in\mathscr{D}, \tag{4.7}$$

where

$$H(\mathbf{x})=\frac{1}{(2\pi)^2}\int\int_{-\infty}^{+\infty}\alpha_{\mathscr{A}}^2(\omega)\exp\left[i(\mathbf{x},\omega)\right]d\omega. \tag{4.8}$$

As usual, K^*K is a self-adjoint, non-negative, compact injective operator in $L^2(\mathscr{D})$, and we denote by α_k its eigenvalues and by u_k the corresponding normalized eigenfunctions. As a consequence there exists for the operator K a singular system $\{\alpha_k^2; u_k, v_k\}_{k=0}^{+\infty}$ such that the set $\{u_k\}_{k=0}^{+\infty}$ is a basis in $L^2(\mathscr{D})$, while the set $\{v_k\}_{k=0}^{+\infty}$ is a basis in $\mathscr{B}_{\mathscr{A}}$. Using this singular system, we can repeat in the two-dimensional case the analysis developed in § 3 for the case of one dimension. In particular, for a given value of the signal-to-noise ratio E/ε, it is possible to determine only those components of the object satisfying condition (3.5).

In order to estimate the resolution achievable by means of the singular value method, we need a numerical computation of the singular values. Such a computation can be done easily only in the case of a square pupil. Since normal pupils are circular this is unfortunate, but it should give some qualitative indication of the effects to be expected.

If we assume that the support of the object is contained in the square $\mathscr{D}=[-X/2, X/2]\times[-X/2, X/2]$, and if we remark that the point-spread function (4.4), as follows from equation (4.2), is given by

$$S(x)=\frac{\sin^2(\Omega x_1)}{\pi\Omega x_2^2}\,\frac{\sin^2(\Omega x_2)}{\pi\Omega x_2^2}, \tag{4.9}$$

then, introducing again the variables $\mathbf{t}=2\mathbf{x}/X$ and $c=X\Omega/2$, we can express the singular functions and singular values of the operator (4.5), (4.9) in terms of the singular functions and singular values of the operator (2.1):

$$\left.\begin{aligned} u_{i,k}(\mathbf{t})&=u_i(t_1)u_k(t_2),\\ v_{i,k}(\mathbf{t})&=v_i(t_1)v_k(t_2),\\ \alpha_{i,k}&=\alpha_i\alpha_k. \end{aligned}\right\} \tag{4.10}$$

Remark that, while the singular value $\alpha_{i,i}$ is non-degenarate, the singular values $\alpha_{i,k}$, $i\neq k$, have multiplicity 2.

Now we denote again by M_S the number of components of the object corresponding to singular values satisfying the condition

$$\alpha_{i,k}=\alpha_i\alpha_k\geqslant\varepsilon/E. \tag{4.11}$$

The area of a resolution element contained in $\mathscr{D}$ is $D_S^2=X^2/M_S$, and the number of resolution elements contained in the Rayleigh area R^2 is

$$\left(\frac{R}{D_S}\right)^2=\left(\frac{\pi}{2c}\right)^2 M_S. \tag{4.12}$$

The quantities M_S and $(R/D_S)^2$ can be computed using the singular values of the operator (2.1), taking into account the multiplicity of the singular values $\alpha_{i,k}$. Results are given in table 3 and represented graphically in figure 4.

Table 3. Number of components, M_S, and corresponding number of resolution elements within the Rayleigh area, $(R/D_S)^2$, restored by the singular value method, as a function of 'signal-to-noise ratio', E/ε; square pupil case.

$\frac{E}{\varepsilon}$	$c=1$		$c=2$		$c=3$		$c=4$		$c=5$	
	M_S	$(R/D_S)^2$	M_S	$(R/D_S)^2$	M_S	$(R/D_S)^2$	M_S	$(R/D_S)^2$	M_S	$(R/D_S)^2$
10^2	8·16	20·1	18·4	11·4	30·4	8·35	46·6	7·18	67·5	6·66
10^4	19·7	48·6	40·0	24·7	64·9	17·8	92·5	14·2	122·4	12·1
10^6	34·7	85·8	65·8	40·6	99·7	27·3	139·1	21·4	182·1	18·0

$\frac{E}{\varepsilon}$	$c=6$		$c=7$		$c=8$		$c=9$		$c=10$	
	M_S	$(R/D_S)^2$	M_S	$(R/D_S)^2$	M_S	$(R/D_S)^2$	M_S	$(R/D_S)^2$	M_S	$(R/D_S)^2$
10^2	88·1	6·04	111·4	5·61	143·2	5·52	172·7	5·26	205·2	5·06
10^4	157·9	10·8	196·7	9·90	236·0	9·10	284·4	8·66	326·9	8·06
10^6	226·4	15·5	275·6	13·9	330·2	12·7	386·5	11·8	450·0	11·1

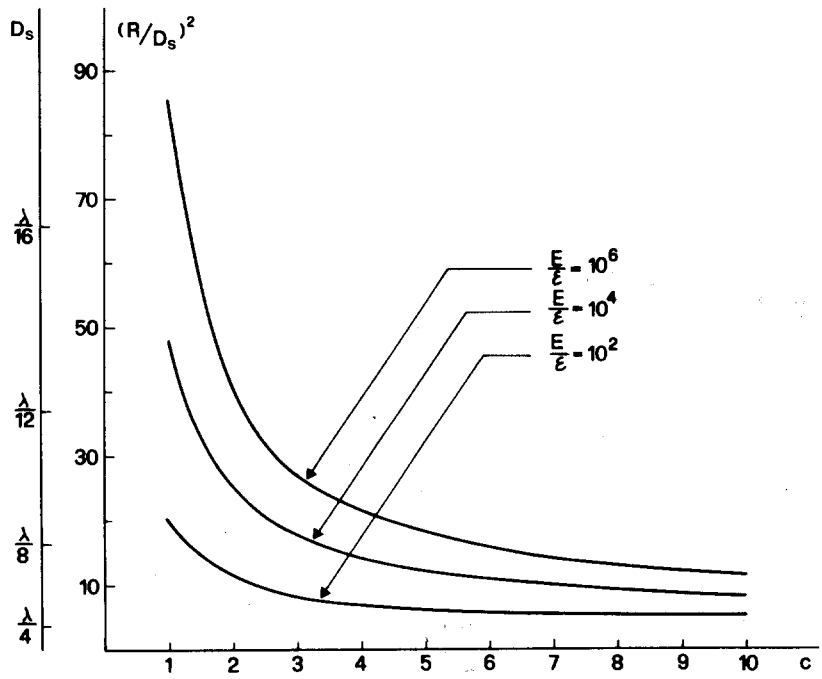

Figure 4. Super-resolution gain using singular value method on complete image for various values of signal-to-noise ratio E/ε. Two-dimensional case, square pupil. The scale on the extreme left shows the linear resolution possible with $R=\lambda/2$.

5. Concluding remarks

As we have shown, super-resolution can be obtained also in the incoherent case when the space-bandwidth product (or equivalently the Shannon number) is small. Therefore all the conclusions derived in [1] can be immediately extended to the present case.

However, a peculiar feature of the incoherent case must be pointed out. Whereas in coherent imaging the singular functions represent physically realizable quantities, for the incoherent case this is true only for the singular functions corresponding to the greatest singular value, since the object and the image cannot both take negative values. The functions defined by equation (3.1) must, therefore, be restricted to combinations of u_k which are everywhere positive. For this reason the relation between resolution and number of degrees of freedom is not so clear as in the coherent case.

For application to microscopy we have the advantage that, contrary to the coherent case, no phase problem exists, but on the other hand, apart from the use of a physical aperture, incoherent objects at low Shannon numbers can be achieved only by self-luminosity or fluorescence. Semiconductor emitters and biological materials tagged with chromophores, respectively, come to mind. For such objects, however, even greater super-resolution gains may be attained than in the coherent case.

Appendix

Let T_c be a self-adjoint Toeplitz operator, i.e.

$$(T_c f)(x) = \int_{-c}^{c} T(x-y) f(y)\, dy, \quad |x| \leqslant c, \tag{A 1}$$

where $T(x)$, $-\infty < x < +\infty$, is a bounded function in $L^1(-\infty, +\infty)$, such that $T^*(x) = T(-x)$. Let $N_c(a, b)$ be the number of eigenvalues of T_c falling within (a, b); if (a, b) does not contain 0 and if $m(a, b)$ is the measure of the ω set where $a < \hat{T}(\omega) < b$, then [6, 7]

$$\lim_{c \to +\infty} \frac{1}{2c} N_c(a, b) = \frac{1}{2\pi} m(a, b), \tag{A 2}$$

provided the sets where $\hat{T}(\omega) = a$ or $\hat{T}(\omega) = b$ are of measure 0.

The previous result can be applied to the operator (1.3), after the change of variable $x = ct$, taking $T(x) = \sin^2(x)/\pi x^2$; in such a case $\hat{T}(\omega)$ is given by equation (1.2) with $\Omega = 1$. Since $\hat{T}(\omega)$ is an even function, it follows that the ω set where $a < \hat{T}(\omega) < b$, $0 < a < b \leqslant 1$, is the union of two intervals, both having a length given approximately by $(\pi/2c) N_c(a, b)$ when c is large. Therefore, if $N_c(a, b) \sim 1$, this length is $\pi/2c$, i.e. one-half the Nyquist distance for the Fourier transform of a function supported in $[-c, c]$. The previous remark implies that, for $k < 4c/\pi$, the eigenvalues are given approximately by the values of $\hat{T}(\omega) = 1 - |\omega|/2$, $|\omega| < 2$, at the sampling points $\omega_k = \pi k/2c$; this result coincides with the approximate formula (1.6). Remark that, in such a case, the number of significant eigenvalues is approximately twice the Shannon number.

Dans un précédent article, les méthodes de développement des fonctions singulières ont été appliquées à l'analyse de l'imagerie cohérente lorsque le domaine de l'image diffère de celui de l'objet. Dans cet article, la méthode est étendue à l'éclairage incohérent, en restreignant l'analyse au cas sans aberration.

Tandis que les fonctions singulières et les valeurs singulières, en imagerie cohérente, sont liées, d'une manière simple, aux fonctions sphéroïdales et à leurs valeurs propres, de telles relations n'existent pas dans le cas de l'imagerie incohérente. En dépit de cette difficulté, un certain nombre de propriétés des fonctions singulières et des valeurs singulières sont établies dans cet article et des estimations asymptotiques sont obtenues dans la limite des grands

produits espace-bande passante. Pour les faibles valeurs de ce produit, les valeurs singulières sont calculées numériquement et, au moyen de ces résultats, on montre que la super-résolution, au sens de l'amélioration des critères précédents en présence de bruit, peut être obtenue.

In einer vorhergehenden Arbeit wurden Entwicklungsverfahren für singuläre Funktionen zur Analyse der kohärenten Abbildung auf den Fall angewandt, daß Objekt- und Bildbereich voneinander abweichen. In der vorliegenden Arbeit wird dieses Verfahren auf die inkohärente Abbildung ausgedehnt, wobei die Analyse auf den aberrationsfreien Fall beschränkt wird.

Während singuläre Funktionen und Werte im Falle kohärenter Abbildung auf einfache Weise mit den Sphäroidfunktionen und deren Eigenwerten zusammenhängen, gibt es keine solchen Zusammenhänge für die inkohärente Abbildung. Trotz dieser Schwierigkeit werden in dieser Arbeit mehrere Eigenschaften der singulären Funktionen und Werte hergeleitet und asymptotische Abschätzungen für den Grenzfall großer Raum-Bandbreiten-Produkte erhalten. Für kleine Werte des Raum-Bandbreiten-Produkts werden die singulären Werte numerisch berechnet und mit Hilfe dieser Ergebnisse wird gezeigt, daß Überauflösung im Sinne von Bildverbesserung bezüglich bekannter Kriterien bei vorliegendem Rauschen erzielt werden kann.

References

[1] Bertero, M., and Pike, E. R., 1982, *Optica Acta*, **29**, 727.
[2] Goodman, J. W., 1968, *Introduction to Fourier Optics* (New York: McGraw-Hill).
[3] Gori, F., 1974, *J. opt. Soc. Am.*, **64**, 1237.
[4] Bendinelli, M., Consortini, A., Ronchi, L., and Frieden, B. R., 1974, *J. opt. Soc. Am.*, **64**, 1498.
[5] Gori, F., and Palma, G., 1975, *J. Phys.* A, **8**, 1709.
[6] Kac, M., Murdock, W. L., and Szegö, G., 1953, *J. rat. Mech. Analysis*, **2**, 767.
[7] Landau, H. J., 1975, *J. Anal. Meth.*, **28**, 335.
[8] Miller, G. F., 1974, *Numerical Solution of Integral Equations*, edited by L. M. Delves and J. Walsh (Oxford: Clarendon Press), p. 175.
[9] Hille, E., and Tamarkin, J. D., 1931, *Acta math.*, **57**, 1.
[10] Hämmerlin, G., and Schumaker, L. L., 1980, *Num. Math.*, **34**, 125.